Effects of magnetic and structural phase transitions on the normal and anomalous Hall effects in Ni-Mn-In-B Heusler alloys

Mikhail Blinov, Anil Aryal, Sudip Pandey, Igor Dubenko, Saikat Talapatra, Valeriy Prudnikov, Erkki Lähderanta, Shane Stadler, Vasiliy Buchelnikov, Vladimir Sokolovskiy, Mikhail Zagrebin, Alexander Granovsky, and Naushad Ali

Phys. Rev. B **101**, 094423 — Published 19 March 2020

DOI: 10.1103/PhysRevB.101.094423

The Effects of Magnetic and Structural Phase Transitions on the Normal and Anomalous Hall Effects in Ni-Mn-In-B Heusler Alloys

Mikhail Blinov[1], Anil Aryal[2*], Sudip Pandey[2], Igor Dubenko[2], Saikat Talapatra[2], Valeriy Prudnikov[1], Erkki Lähderanta[3], Shane Stadler[4], Vasiliy Buchelnikov[5], Vladimir Sokolovskiy[5], Mikhail Zagrebin[5], Alexander Granovsky[1], and Naushad Ali[2]

[1]Faculty of Physics, Lomonosov Moscow State University, Moscow, 119991 Russia
[2]Southern Illinois University, Department of Physics, Carbondale, Illinois, United States
[3]Lappeenranta University of Technology, 53851, Finland
[4]Louisiana State University, Department of Physics and Astronomy, Baton Rouge, LA, United States
[5]Chelyabinsk State University, 454001, Chelyabinsk, Russia

Abstract

Magnetization, electrical resistivity, magnetoresistance, and Hall resistivity of $Ni_{50}Mn_{35}In_{14.25}B_{0.75}$ and $Ni_{50}Mn_{35}In_{14.5}B_{0.5}$ Heusler alloys were studied in a temperature range T = 80-400 K in magnetic fields up to 20 kOe. Both alloys exhibit a martensitic transformation from a high-temperature ferromagnetic austenite phase to a low-temperature, low-magnetization martensitic phase. The electrical resistivity nearly doubles as a result of the martensitic transformation, reaching 180 and 100 μΩcm in the martensitic states of $Ni_{50}Mn_{35}In_{14.25}B_{0.75}$ and $Ni_{50}Mn_{35}In_{14.5}B_{0.5}$, respectively. The temperature dependence of the electrical resistivity does not corresponded with the Mooij correlation. The magnetoresistance is negative with a narrow negative peak at the martensitic transition. Normal and anomalous Hall effect coefficients were determined by fitting the field dependencies of the Hall resistivity using magnetization data. The coefficients of the normal Hall effect for both compositions were found to decrease with temperature from positive values in the austenite to negative values in the martensite phase. None of the known correlations between the anomalous Hall effect coefficient and resistivity were satisfied. Significant changes in the values of the anomalous Hall coefficients during the martensitic transformation are explained by the difference in spin-up and spin-down state

occupations in the martensite and austenite phases. First-principle calculations of the electronic structures confirm this explanation.

*) corresponding author: aryalanil@siu.edu

1. Introduction

The anomalous Hall effect (AHE) has been attracting continuous attention for almost 140 years. A long time after its discovery, even a qualitative explanation of the origin of this effect has not been offered. Studies of the AHE in low-resistivity ferromagnetic alloys have made it clear that this phenomenon can be associated with effects of spin-orbit interactions (SOI) on spin-polarized charge carriers [1]. The basic theory of the AHE was developed by Smith, Karplus, Luttinger, and Berger who formulated three main competitive mechanisms, namely, an intrinsic or Karplus-Luttinger mechanism, subsequently interpreted through the Berry phase, skew scattering, and side-jump scattering (see review [1] and references therein). However, the dominant mechanism is still under debate (for example [1-7]).

As one of the first effects associated with spin-dependent scattering and SOI, the AHE turned into a developing factor regarding a new generation of electronics such as spintronics and spin-orbitronics. In spite of the whole family of Hall effects (direct and inverse spin Hall effects, quantum anomalous, topological, tunneling, and optical Hall effects, etc.), having the same spin-orbit origin, the mechanisms responsible for AHE behavior in different systems are not clear and requires detailed studies.

It is widely believed the AHE in highly resistive metals is due to intrinsic mechanisms and side jumps. The both mechanisms result in the linear dependency of the AHE coefficient (R_s) on the square of the resistivity (ϱ) [1]. However, in many cases, particularly in disordered transition metal alloys and composites (see examples in [2-7]), this is not the case. Striking representatives of such highly resistive metals are Heusler alloys with resistivities greater than

100-150 μΩcm, in which the correlation $R_s \sim \varrho^2$ was found to not be satisfied [2-5,7]. Some of the Heusler alloys provide an ideal platform for studying AHE behavior in highly resistive systems, since different phase transitions, including magnetic and magnetostructural transitions, accompanied by drastic changes in resistivity, can be observed for the same composition. On the other hand, the study of contributions from the normal Hall effect (NHE) and the AHE to the total Hall effect may be useful for elucidating the mechanisms driving the magnetostructural transitions, in particular, to what extent the electronic structure changes in such a transition. This seems to be important in connection with the understanding of the mechanisms of the martensitic and magnetostructural transitions in magnetocaloric materials [8, 9]. However, a study of both the martensitic and austenitic phases, with a consistent consideration of the NHE and AHE contributions, has not yet been performed. In this work, polycrystalline $Ni_{50}Mn_{35}In_{14.25}B_{0.75}$ and $Ni_{50}Mn_{35}In_{14.5}B_{0.5}$ alloys were chosen for study. The martensitic transitions (MT) in these alloys occur below or in close vicinity to room temperature. This makes it possible to study the Hall effect in the ferromagnetic and weakly magnetic martensitic phase (MP), in the paramagnetic and ferromagnetic austenitic phase (AP), and directly at the magnetostructural transition (MST).

2. Experimental

2.1 Samples

Polycrystalline $Ni_{50}Mn_{35}In_{14.25}B_{0.75}$ and $Ni_{50}Mn_{35}In_{14.5}B_{0.5}$ samples were prepared using 4N-purity elements by arc-melting in an argon atmosphere. The samples were wrapped in tantalum foil and annealed at 850°C for 48 hours under vacuum and then slowly cooled down to room temperature. The phase compositions and crystal structures were studied by powder X-ray diffraction (the results are shown in Fig. 1). Complicated X-ray diffraction patterns were observed for all samples and identified as a mixture of high-temperature cubic (austenitic) and low-temperature orthorhombic (martensitic) phases of different ratios for different samples.

2.2 Magnetic and transport properties measurements

The physical properties (magnetization, resistivity, etc.) were measured after the samples were cooled down to 80 K from 400 K in zero magnetic field (ZFC), and in the presence of a magnetic field during heating (FC), and also during cooling in field from 400 K to the final temperature (FCC protocol). Magnetization, resistance, magnetoresistance, and Hall resistance measurements were conducted using the same samples of approximate dimensions 5×1.5×0.5 mm^3. The magnetic properties were studied using a LakeShore vibrating sample magnetometer in magnetic fields up to 16 kOe. Temperature dependencies of the magnetizations, M(T) curves, were investigated during heating (ZFC) from 80 K to 400 K and subsequent cooling (FCC) in an applied magnetic field of 16 kOe applied parallel to plane of the samples. Magnetization versus field measurements were conducted at constant temperature in out-of-plane field orientations similar to that used for transport measurements. Electrical resistance measurements were made were measured using a four-probe method during cooling and heating procedures (ZFC). Magnetoresistance (MR) and Hall resistance measurements were carried out at constant temperatures during magnetic field changes up to 20 kOe.

The Hall resistivity ρ_H is described by the sum of two terms:

$$\rho_H = R_0 B + 4\pi R_s M \,, \tag{1}$$

where the first term represents the normal Hall effect (NHE) induced by the Lorentz force and the second term characterizes the AHE related to SOI. M is the magnetization component perpendicular to the sample plane, B is the magnetic induction component in this direction, and R_0 and R_s are NHE and AHE coefficients, respectively. The conventional method of separating the NHE and AHE contributions from the field dependence of the $\rho_H(H)$ below the Curie temperature is based on the assumption that $R_s >> R_0$. This is true in most cases, and it is therefore straight forward to determine both coefficients through the linearization of the low field and high field parts of the curve $\rho_H(H)$. However, this method is not appropriate for the Heusler alloys above the Curie temperature, and also in low magnetization states of the MP, where the second term in Eq.1 can be of the same order of magnitude as the first. Therefore, to determine

R_0 and R_s we fit the $\rho_H(H)$ curves in the full magnetic field range using magnetization data while considering R_0 and R_s, as fitting parameters. This method is equivalent to that considered above if the second term in Eq.1 is much larger than the first, but it is also valid if this is not the case.

3. Results and Discussion

Fig.2 shows the FC and FCC magnetization (M(T)) measurements for the $Ni_{50}Mn_{35}In_{15-x}B_x$ samples at H=16 kOe. Three temperature induced phase transitions at T_{CM}, T_A/T_M, and T_C can be clearly seen in the magnetization curves. Based on the FC M(H) magnetization curves (Figs. S1 and S2 [10]), the phase transitions have been described as follows: i) a ferromagnetic martensitic (FMM) transition to a low magnetization (weak ferromagnetic or paramagnetic with antiferromagnetic correlations) martensitic state (LMMS) at T_{CM}; ii) an inverse MT at T_A from a LMMS to a ferromagnetic/paramagnetic austenitic state (FMA/PMA) and a direct MT at T_M; and iii) a transition from a FMA to PMA at T_C. Temperature hysteresis is observed in both samples in the vicinity of T_A/T_M, indicating a first order MT at approximately 250 K and 300 K for x=0.75 and 0.5, respectively. The ferromagnetic MP is characterized by a complicated magnetic structure that results in exchange bias phenomena at low temperature (not shown) [see for example in Ref. 11].

Figs. 3 and 4 summarize the magnetotransport data for $Ni_{50}Mn_{35}In_{14.25}B_{0.75}$ and $Ni_{50}Mn_{35}In_{14.5}B_{0.5}$, respectively. Details of MR and Hall effect resistivity field dependencies, as well as fitting curves used for determination Hall coefficients R_0 and R_s, are given in Figs. S3-S7 [10]. Electrical resistivity is presented for both cooling and heating, while magnetoresistance (MR) and Hall effect data are shown for cooling only due to the fact that cooling provides a large temperature region of AP stability (see in Fig. 2).

The thermal hysteresis of the $Ni_{50}Mn_{35}In_{14.25}B_{0.75}$ resistivity (Fig.3a) corresponding to the MT is easily identified. The resistivity of the sample increases slightly with temperature above and below of the MT and decreases drastically by about a factor three during the MT, namely at the transition from the MP to the AP (shown in Figure 3a). Such a significant change in the

resistivity and field-induced shift of the MT transition to the low temperature region leads to a large MR. A change in magnetic field of 20 kOe results in -11% MR at 246 K (Fig.3b).

Fig.3c shows the temperature dependence of the NHE and AHE coefficients for $Ni_{50}Mn_{35}In_{14.25}B_{0.75}$. The NHE changes sign from negative in the MP to positive in the AP at ~240 K, and this temperature coincides well with the MT. Thus, the dominating current carriers in $Ni_{50}Mn_{35}In_{14.25}B_{0.75}$ are electrons and holes for the MP and AP, respectively, and the electronic structure changes during the MT. The AHE coefficient increases with temperature in the MP with a significant drop during the MT. The AHE coefficient at 300 K in the AP is approximately 2-3 times smaller than at low temperature in the MP.

The resistivity of $Ni_{50}Mn_{35}In_{14.5}B_{0.5}$ (Fig.4a) shows behavior nearly identical to that of $Ni_{50}Mn_{35}In_{14.25}B_{0.75}$, although with a significantly narrower thermal hysteresis. A hysteresis of about 0.5 K was detected at the MT. The slight discrepancy in the resistivity values for cooling and heating outside of the MT temperature range may be related to some heat transfer lag between the thermosensor and the sample during continuous measurement of the resistance. The MR reaches -11% at the temperature of the MT at H=20 kOe (Fig.4b). Another local minimum can be observed at a higher temperature (315 K), which is attributed to the transition between the paramagnetic and ferromagnetic states.

The NHE and AHE coefficients for $Ni_{50}Mn_{35}In_{14.5}B_{0.5}$ follow the same tendency as for $Ni_{50}Mn_{35}In_{14.25}B_{0.75}$. The NHE coefficient changes sign during the MT, the AHE coefficient increases with temperature in the MP and decreases during the inverse MT. A large part of the AP falls into paramagnetic state. The paramagnetic state has significantly lower magnetization and Hall resistivity values, leading to an increase in computational error during the Hall fitting procedure in this temperature range.

Discussion

The electrical resistivities in both systems show similar behaviors that are typical for Heusler alloys undergoing an MST [4]. Namely, the resistivity is large in the MP and sharply

decreases during the transition to the AP. There are three possible reasons for the decrease in the resistivity in the AP. Firstly, the crystal structure of the AP is more symmetric, and a smaller scattering intensity should therefore be expected. Secondly, there may be a significant change in the density of electronic states at the Fermi level during the MT. Thirdly, during the transition to the AP, the scattering by the MP twins disappears. It is likely that all three mechanisms are significant in the case of Heusler alloys. In the AP, the temperature dependence of the resistivity is conventional for ferromagnetic metals: the resistivity increases with temperature due to scattering by phonons and spin fluctuations, and at the Curie temperature the slope of the temperature curve changes. Interestingly, according to the X-ray data (Fig. 1), the alloy with x=0.75 at 300 K is inhomogeneous as it contains only 74% of the AP, but the temperature dependence is the same as in homogeneous ferromagnets.

Three striking features should be mentioned for these alloys. First, the resistivity of the MP of the alloy with x=0.75 is about 1.8 times greater than that for x=0.5. Second, for the alloy with x=0.75 the resistivity increases in the MP with temperature up to the transition to AP; for the alloy with x = 0.5, the initial growth is replaced by a decrease in resistance starting from 200 K. Finally, no signs of magnetic phase transitions have been observed near T_{CM} for either alloy. The first feature is closely related to reports in the literature of extreme sensitivity of the electronic structure of the Ni-Mn-In based Heusler alloys to small deviations from stoichiometry and chemical composition [11]. It can also be clearly seen from the data on the NHE, whose coefficients in these alloys differ by several multiples. In spite of the behavior being characteristic of the Heusler alloys, such large differences in the Hall constant resulting from just a 0.25% B doping concentration is unusual. It is most likely related to large local distortions resulting from the difference in sizes of the B and In-atoms.

The temperature dependencies of the resistivity require a more detailed discussion. Indeed, according to the Mooij rule [12], the resistivity of highly resistive alloys with residual resistivities above 150 μΩcm should decrease with increasing temperature, whereas in the alloy with x=0.75 it grows monotonically in the MP (see Fig. 3a). This means that the Mooij rule does

not apply in the case of x=0.75 below T_{CM}. Apparently, the decrease in resistivity with an increase in temperature in non-magnetic high-resistive alloys with a strong degree of disorder is due to the fact that ion oscillations reduce the degree of disorder in the alloy, but the scattering by spin fluctuations increases with temperature up to the Curie temperature, independent of structural disorders as in the case of low-resistive alloys. This provides a way to explain the violation of the Mooij rule in disordered ferromagnetic alloys.

More complex behavior is observed in the alloy with x=0.5 (Fig.4). The resistance is almost constant up to 200 K and then begins to decrease, although the transition to the AP occurs around 300 K. We attribute this to two things. First, the temperature-induced first order phase transition is characterized by phase co-existence region. In this region the high and low temperature phases co-exist with a strong temperature dependence of the phase ratio. That is, the alloy is a composite of high resistivity martensite and austenite with a significantly smaller resistivity than the martensite. Therefore, increasing the amount of austenite inclusions in the MP leads to a decrease in resistivity. The second reason is the change of electronic structure. The change in the sign observed for the NHE (Fig. 3) shows a transition from electron to hole conductivity in the same temperature region.

It is necessary to emphasize here that the transitions observed in the MP are not the usual homogeneous ferromagnetic-paramagnetic transitions, but transitions between a ferromagnetic and a low magnetization state (see Fig. 2a). Thus, the absence of evidence of magnetic phase transitions in the temperature behavior of the resistivity in the MP is related to nature of such transitions. The same is true for the MR behaviors. The MR exhibits negative peaks at the MT and at the Curie temperature of the AP (Figs.3 and 4) and does not show changes in the vicinity of T_{CM}. Magnetic transitions in the MP are blurred in temperature, and the presence of antiferromagnetic correlations smoothes the resistivity and MR behavior. The exchange bias phenomena that have been observed for such alloys below T_{CM} confirm that the compounds can be considered to possess an inhomogeneous ferromagnetic-antiferromagnetic structure.

The most interesting results were observed for the magnitude and temperature dependence of the AHE coefficient. For the alloy with x=0.5, R_S= 3.5 10^{-10} ΩcmG and ρ= 100 μΩcm and T=225 K. However, for x=0.75 at the same temperature, R_S=1 10^{-10} ΩcmG, i.e., several times less, although the resistivity is 1.8 times greater than observed for x=0.5. That is, the correlation between the magnitudes of R_S and ρ^2 does not take place (the difference is more than an order of magnitude). Further, for an alloy with x=0.5 in the temperature range of 200-300 K, the resistivity decreases, while R_S increases. Thus, both in terms of magnitude and temperature dependence, the correlation of R_S and ρ^2 is not present. Plotting the AHE coefficient versus electrical resistivity on a logarithmic scale allows the derivation of a power coefficient in the relation R_S versus ρ^{α}. In the case of x= 0.75 it was found that α=1.4 ±0.1 in the MST range and 4.6 ± 3.8 for the AP (Fig. S5). The relative fitting error of 82% is drastic. In the MP, the parameter α is even negative with higher relative fitting errors. This result is not unexpected, as it has already been observed for other Heusler alloys [2-5, 7] and we have previously noted that there is no universal correlation between R_S and ρ in the case of inhomogeneous systems.

In previously studied Heusler alloys, the change in R_S in the vicinity of the MST is small and monotonic. There were also no sharp changes in R_0 [2-4]. This serves as proof that the electronic structures of the alloys change slightly near the MST, which was confirmed by electronic heat capacity data [13] and magneto-optical spectra [14], and did not contradict the results of theoretical calculations of the electronic structures. Moreover, the analysis of the magnetocaloric effect in metamagnetic Heusler alloys is also based on negligible changes in the electronic contribution to the entropy during the MST [8,9]. In contrast to previous studies, in the present investigation R_S varies greatly during the transition from the martensite to the austenite phases and increases significantly with temperature in the MP.

Now consider the possible causes of such behavior. If we assume that Heusler alloys are composites containing a high-resistive martensitic and low-resistive austenitic phase characterized by their respective values of R_S and ρ, the increase in the amount of austenite

cannot lead to an increase in R_S in the MP, but only to a decrease in R_S [15]. So the interpretation as a mixture of two phases does not work. Second, the increase in R_S with temperature in the MP cannot be associated with an increase in the scattering intensity because the resistivity of the alloy with x=0.5 does not increase in this temperature range. Third, using an analogy with nanogranular alloys [16] and assuming the formation of AF nanogranules inside the MP with enhanced SOI at the interfaces, it is possible to explain the increasing Rs in the MP while approaching the MT, and its decrease when the homogeneous AP appears. But this mechanism of SOI enhancement on interfaces between the AP and MP phases should work for all metamagnetic Heusler alloys, not for only those studied in the present investigation.

We offer the following explanation, which does not contradict most available data. The conductivity of an alloy is determined by the sum of the conductivity of states with spin-up and spin-down electrons, $\sigma = \sigma\uparrow + \sigma\downarrow$, and these conductivities are of the same sign for both electrons and holes. The anomalous Hall effect conductivity, which is proportional to the AHE coefficient, $\sigma a = \sigma a\uparrow + \sigma a\downarrow$, is also the sum of Hall conductivities with opposite spin polarizations, but the signs of these contributions for electrons and holes are opposite. Therefore, even with minor changes in the electronic structure, in which the total density of states at the Fermi level varies slightly, strong changes in the σa are possible if one of the subbands is shifted in energy at the MST. Moreover, the sign of the contribution of one of the spin subbands, for example $\sigma a\downarrow$, can change during the transition from electron to hole conductivity, since this sign also depends on the type of carrier [17]. This change of the conductivity type in the alloys under study really takes place according to the data on the NHE. It should also be noted that the carriers for normal and AHE conductivities can belong to different groups of carriers, since the SOI responsible for the AHE is most pronounced for carriers of narrow bands. We carried out first-principle calculations of the electronic structures of $Ni_2Mn_{1.4}In_{0.6-x}B_x$ (x=0.0-0.03) alloys at T=0 and the results confirm quite large changes of the ratio between spin-up and spin-down states for the total and d-orbital resolved density of states at the Fermi level for the austenite and martensite (see Figs.S6-S9 and Table

S1 in Supplemental Material [10]) (see, also, Ref. [18-23] therein). In fact, the calculated ratio of spin-up to spin-down states in the martensite is approximately twice that of the austenite.

Conclusions

Magnetic and magnetotransport properties of $Ni_{50}Mn_{35}In_{14.25}B_{0.75}$ and $Ni_{50}Mn_{35}In_{14.5}B_{0.5}$ Heusler alloys were studied in a wide temperature range and both the NHE and AHE coefficients were determined in the ferromagnetic MP, the low magnetization MP, in the vicinity of the MST, and in the ferromagnetic and paramagnetic AP. There are characteristic kinks/negative peaks in temperature dependencies of the resistivity/magnetoresistance at the magnetic phase transition in the AP at the Curie temperature, but not in the MP. This indicates that the magnetic phase transition from the ferromagnetic to low magnetization state in the MP is smeared due to magnetic inhomogeneity. It was shown that the Mooij criterion does not apply in the MP, which is explained by the increasing role of scattering by spin fluctuations. There is no universal correlation between the AHE coefficient and the electrical resistivity, either in their values or in their temperature dependencies. The NHE coefficient changes sign at the MST, which is direct evidence of an electronic structure transformation, but these changes are small and monotonic. The AHE coefficient changes much more strongly at the MST. We propose that this effect is due to a high AHE sensitivity to small variations in the occupation of spin-up and spin-down states at the Fermi level since these states give AHE contributions that are opposite in sign.

Acknowledgment:

This work was supported by the U.S. Department of Energy (DOE), Office of Science, Basic Energy Sciences Award No. DE-FG02-06ER46291 (SIUC) and DE-FG02-13ER46946 (LSU), by the Academy of Finland, grant No. 318405 (LU Technology); M. I. Blinov acknowledges support from the Foundation for the Advancement of Theoretical Physics “BASIS” (Russia).

.

References

[1] N. Nagaosa, J. Sinova, S. Onoda, A. H.MacDonald, and N. P. Ong, Rev. Mod. Phys. **82**, 1539 (2010).

[2] A. B. Granovskii,, V. N. Prudnikov, A. P. Kazakov, A. Zhukov, and I. Dubenko, JETP **115** (5) 805 (2012).

[3] S.Pandey, M. Blinov, A. Aryal, I. Dubenko, V. Prudnikov, E. Lahderanta, A. Granovsky, N. Kazachkova, S. Stadler, N. Ali, J. Magn. Magn. Mater. **481** 25 (2019).

[4] I. Dubenko, N. Ali, S. Stadler, A. Zhukov, V. Zhukova, B. Hernando, V. Prida, V. Prudnikov, E. Ganshina, and A. Granovsky, Chapter II in hard book: Novel Functional Magnetic Materials: Fundamentals and Applications (ed. A. Zhukov), Springer, *Series in Materials Science* **231**, (2016) pp. 41-83.

[5] J.Kaštil, J.Kamarád, M.Míšek, J.Hejtmánek, Z.Arnold, J. Magn. Magn. Mater. **466** 260 (2018).

[6] A. B. Pakhomov, X. Yan, and B. Zhao, Appl. Phys. Lett. **67**, 3497 (1995).

[7] V. V. Khovaylo, T. Omori, K. Ando, X. Xu, and R. Kainuma, A. P. Kazakov, V. N. Prudnikov, E. A. Gan'shina, A. I. Novikov, Yu. O. Mikhailovsky, D. E. Mettus, and A. B. Granovsky, Phys. Rev. B **87**, 174410 (2013).

[8] T. Gottschall, A. Gracia-Condal, M. Fries, et al., Nat. Mater. 17 (2018) 929.

[9] V. Franco, J.S. Blázquez, J.J. Ipus, J.Y. Law, L.M. Moreno-Ramírez, A. Conde, Progress in Materials Science **93** 112 (2018)

[10] See Supplemental Material at [URL will be inserted by the production group] for M(H) curves, magnetic field dependencies of MR, Hall resistivity and its fittings, and first-principle calculations of electronic structure (which includes Refs. [18-23])

[11] A. K. Pathak, M. Khan, B. R. Gautam, S. Stadler, I. Dubenko, N. Ali, *Exchange bias in bulk Ni–Mn–In-based Heusler alloys*, J. Magn. Magn. Mat., **321** (2009) 963-965. DOI: 10.1016/j.jmmm.2008.03.008.

[12] J.H. Mooij, Phys. State Sol (a) **17**, 521 (1973).

[13] T. Kihara, X. Xu, W. Ito, R. Kainuma, M. Tokunaga, Phys. Rev. B **90** 214409. (2014).

[14] A. Novikov, A. Sokolov, E.A. Gan'shina, et al., J. Magn. Magn. Mater. **432** (15) (2017).

[15] A. B. Granovsky, A. V. Vedyayev, and F. Brouers, J. Magn. Magn. Mater. **136**, 229 (1994).

[16] A. Granovsky, F. Brouers, A. Kalitsov, M. Chshiev, J. Magn. Magn. Mater. **166,** 193 (1997).

[17] E. Kondorskii, Sov. Phys. JETP 28 (2), 291 (1969).

[18] G. Kresse and J. Furthmüller, Phys. Rev. B **54**, 11169 (1996).

[19] G. Kresse and D. Joubert, Phys. Rev. B **59**, 1758 (1999).

[20] J. P. Perdew, K. Burke, and M. Ernzerhof, Phys. Rev. Lett. **80**, 891 (1998).

[21] H. J. Monkhorst and J. D. Pack, Phys. Rev. B **13**, 5188 (1976).

[22] H. Ebert, D. Ködderitzsch, J. Minár, Rep. Prog. Phys. **74**, 096501 (2011).

[23] C.G. Broyden, Math. Comp. **19**, 577-593 (1965).

Figure Captions:

Figure 1 Room temperature XRD patterns for $Ni_{50}Mn_{35}In_{15-x}B_x$, with x=0, 0.5, and 0.75. The Miller indices are shown in brackets. A_{MP} and A_{AP} denote the martensitic and austenitic phase fractions, respectively.

Figure 2: Temperature dependence of the magnetization of $Ni_{50}Mn_{35}In_{14.25}B_{0.75}$ and $Ni_{50}Mn_{35}In_{14.5}B_{0.5}$ at a magnetic field of 16 kOe during heating from 80 K (open symbols) and cooling from the paramagnetic state (400 K) (closed symbols).

Figure 3 (a) The temperature hysteresis of the resistivity obtained at μ_0H=0T; The directions of the temperature changes are shown by arrows. (b) The magnetoresistance during cooling for magnetic field changes of $\Delta\mu_0H$= 2 T (c) NHE (R_0) and AHE (R_S) coefficients during cooling.

Figure 4 (a) Electrical resistivity during heating and cooling obtained at H=0. (b) Magnetoresistance during cooling for a magnetic field change of $\Delta\mu_0H$=20 T. (c) NHE (R_0) and AHE (R_S) coefficients during cooling. The directions of temperature changes, and T_C and T_{CM}, are shown by arrows.

Figs

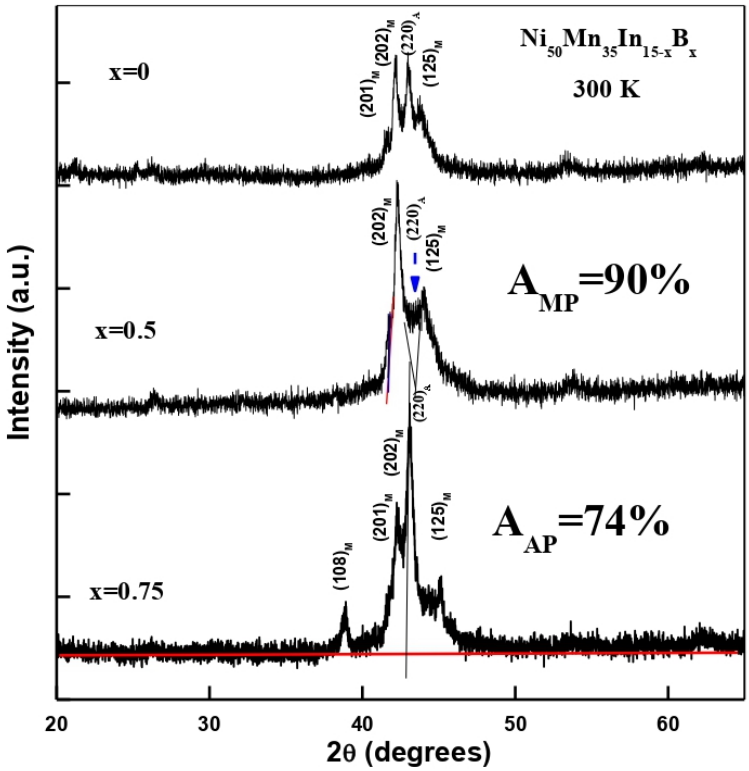

Figure 1 Room temperature XRD patterns for $Ni_{50}Mn_{35}In_{15-x}B_x$, with x=0, 0.5, and 0.75. The Miller indices are shown in brackets. A_{MP} and A_{AP} denote the martensitic and austenitic phase fractions, respectively.

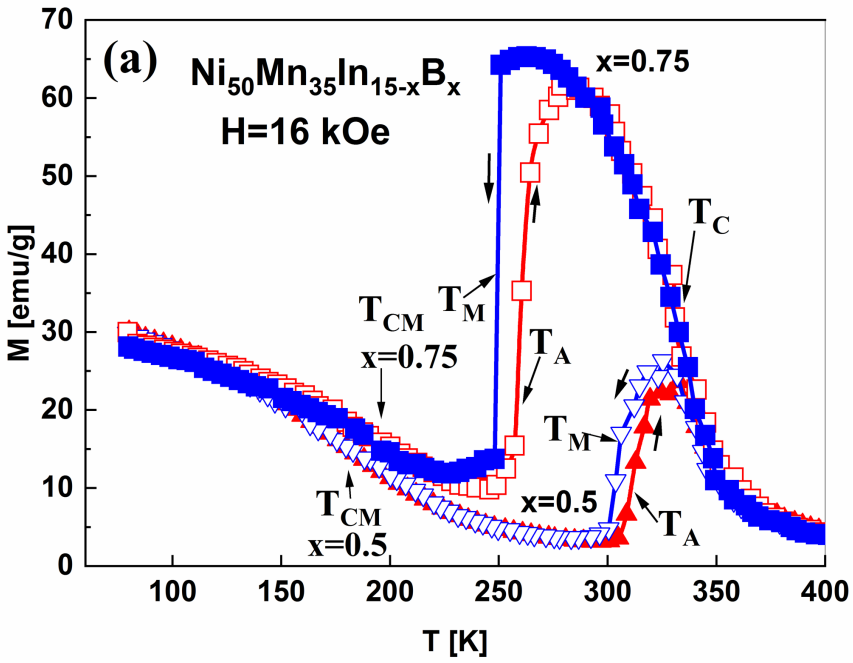

Figure 2: Temperature dependence of the magnetization of $Ni_{50}Mn_{35}In_{14.25}B_{0.75}$ and $Ni_{50}Mn_{35}In_{14.5}B_{0.5}$ at a magnetic field of 16 kOe during heating from 80 K (open symbols) and cooling from the paramagnetic state (400 K) (closed symbols).

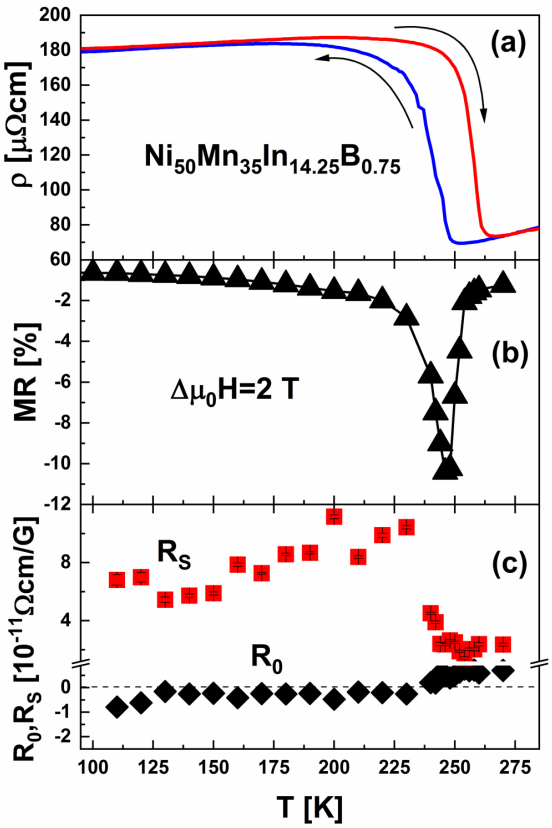

Figure 3 (a) The temperature hysteresis of the resistivity obtained at $\mu_0 H$=0T; The directions of the temperature changes are shown by arrows. (b) The magnetoresistance during cooling for magnetic field changes of $\Delta\mu_0 H$= 2 T (c) NHE (R_0) and AHE (R_S) coefficients during cooling.

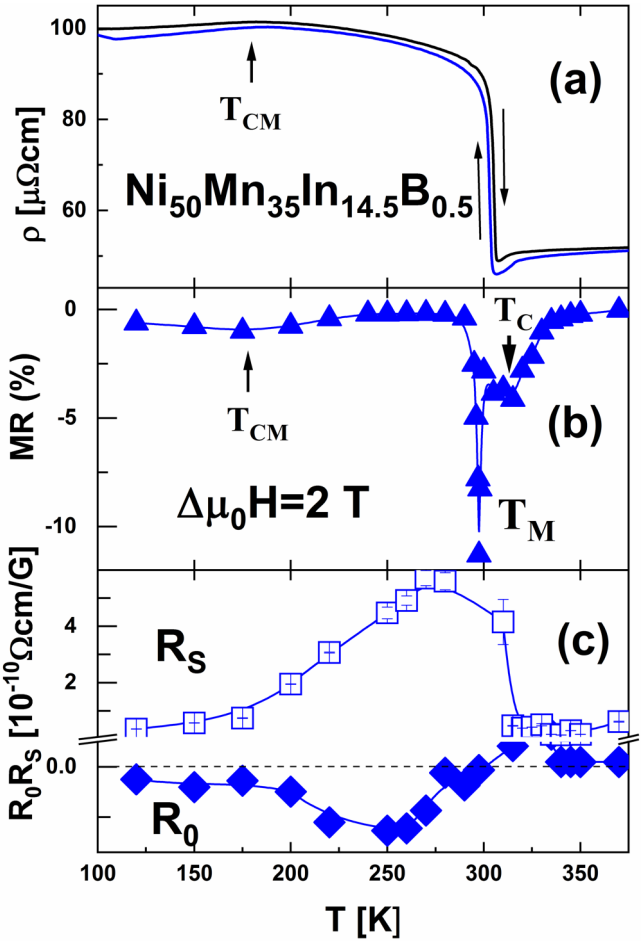

Figure 4 (a) Electrical resistivity during heating and cooling obtained at H=0. (b) Magnetoresistance during cooling for a magnetic field change of $\Delta\mu_0 H$=20 T. (c) NHE (R_0) and AHE (R_S) coefficients during cooling. The directions of temperature changes, and T_C and T_{CM}, are shown by arrows.